JLB

Article

Uterine natural killer cell partnerships in early mouse decidua basalis

Allison M. Felker and B. Anne Croy

Department of Biomedical and Molecular Sciences, Queen's University, Kingston, Ontario, Canada

RECEIVED MAY 26, 2015; REVISED FEBRUARY 8, 2016; ACCEPTED FEBRUARY 23, 2016. DOI: 10.1189/jlb.1HI0515-226R

ABSTRACT

The decidua basalis of developing mouse implantation sites is highly enriched in CD45$^+$ leukocytes. In intact, syngeneically mated C57BL/6 decidua basalis examined at gestation day 8.5 by whole-mount in situ immunohistochemistry, leukocyte, but not trophoblast, conjugations were reported. Nothing is known regarding time course, frequency, composition, or importance of physiologic decidual CD45$^+$ cell pairing. In this study, we confirmed the presence of anti-CD54$^+$/anti-CD11a$^+$ immune synapses in CD45$^+$ decidual cell conjugates and characterized their cellular heterogeneity. Conjugated cell pairs were virtually absent before implantation (virgin and gestation days 3.5 and 4.5), were infrequent at gestation day 5.5, but involved 19% of all CD45$^+$ cells by gestation day 8.5, then declined. By gestation day 8.5, almost all CD45$^+$ cells coexpressed CD31, and 2 CD45$^+$CD31$^+$ cells composed most conjugates. Conjugation partners were defined for 2 nonoverlapping uterine natural killer cell subsets (Ly49C/I$^+$/*Dolichos biflorus* agglutinin lectin$^-$ and Ly49C/I$^-$/*Dolichos biflorus* agglutinin lectin$^+$). Ly49C/I$^+$ uterine natural killer cells were the major subset from before mating up to gestation day 6.5. At gestation day 5.5/6.5, uterine natural killer cell conjugates involving Ly49C/I$^+$ cells were more abundant. By gestation day 8.5/9.5, *Dolichos biflorus* agglutinin lectin$^+$ uterine natural killer cells were the dominant subset with *Dolichos biflorus* agglutinin lectin$^+$/*Dolichos biflorus* agglutinin lectin$^+$ homologous conjugates and *Dolichos biflorus* agglutinin lectin$^+$/*Dolichos biflorus* agglutinin lectin$^-$ heterologous conjugates dominating uterine natural killer cell pairings. At gestation day 6.5, both Ly49C/I$^+$/CD45$^+$ and *Dolichos biflorus* agglutinin lectin$^+$/CD45$^+$ heterologous conjugate pairs strongly engaged antigen-presenting cells (CD11c$^+$, CD68$^+$, or major histocompatibility complex class II$^+$). By gestation day 8.5, dominant partners of Ly49C/I$^+$/CD45$^+$ and *Dolichos biflorus* agglutinin lectin$^+$/CD45$^+$ heterologous conjugates are T cells (CD8$^+$ >CD4$^+$). Heterologous conjugates that did not involve uterine natural killer cells occurred but did not suggest antigen presentation to T cells. These data identify gestation day 6.5–8.5 in the pregnant mouse as a critical window for leukocyte interactions that may establish immune regulation within implantation sites. *J. Leukoc. Biol.* 100: 645–655; 2016.

Abbreviations: B6 = C57BL/6 mouse, DBA lectin = *Dolichos biflorus* agglutinin lectin, DC = dendritic cell, gd = gestation day, IF = immunofluorescence, IHC = immunohistochemistry, ILC = innate lymphoid cell, PAS = periodic acid-Schiff, PFA = paraformaldehyde, uNK = uterine NK, WM-IHC = whole mount in situ immunohistochemistry

The online version of this paper, found at www.jleukbio.org, includes supplemental information.

Introduction

Endometrial decidualization accompanies embryo implantation in species with hemochorial placentation, including humans and mice. Almost half the cells in the developing microdomain, called the decidua basalis, are CD45$^+$ leukocytes, among which highly proliferative [1, 2] uterine NK cells are the most enriched, expanding cell lineage [3, 4]. Other leukocyte lineages within the decidua basalis are less frequent and stable in proportion between gd 5.5–9.5 [4]. Major MHCII$^+$ APCs, macrophages, and DCs each represent ~15–20% of all CD45$^+$ cells [4–8]. Less frequent leukocyte lineages include CD4$^+$ and CD8$^+$ T cells (<2% each) [4, 9].

Not only is the overall pattern of CD45$^+$ cell frequency consistent over early pregnancy [4, 8], but predictable dynamic changes occur within lineage subsets. Histologically, 2 distinct subsets of uNK cells develop within the mouse decidual basalis that are distinguished by reactivity with DBA lectin. DBA$^+$ and DBA$^-$ uNK cells appear to be functionally distinct [10–12] and differ from circulating NK cells, because their differentiation is independent of the transcription factor NFIL3 (E4BP4) [13] (unpublished results). Flow cytometry of decidual cell suspensions identified multiple uNK cell subsets. In mice of C57BL/6 (B6) background, CD122$^+$ uNK cell subsets can be distinguished by their reactivity with NK1.1 and DBA. NK1.1$^-$CD122$^+$DBA$^+$ uNK cells appear to be unique to the decidua and are functionally biased toward regulation of angiogenesis [10, 14, 15]. They are absent from virgin and preimplantation uteri (implantation occurs at gd 4.0–4.5 in mice) [16–18]. Uterine NK1.1$^+$CD122$^+$DBA$^-$ cells are present before implantation and decidualization [18, 19], are more similar to splenic NK cells [11], and produce most of the IFN-γ found in the decidua basalis [10, 20]. IFN-γ is critical for physiologic modification of maternal spiral arteries, a process

Correspondence: Allison M. Felker, Department of Biomedical and Molecular Sciences, Queen's University, Kingston, ON Canada K7L 3N6.
E-mail: a.felker@queensu.ca

completed between gd 9.5–12.5 in mice [20, 21]. Spiral arteries are the major conduits that bring nutrient-rich maternal blood toward the placental labyrinth, the maternal–fetal exchange area within the placenta that is present from gd 10.5 onward [22, 23].

Although many researchers have postulated that uNK cells interact with placentally derived trophoblasts that invade the maternal decidua basalis during its development [24, 25], our studies of live, intact implantation sites at the time of implantation and early afterward (gd 4.5–8.5) do not support that hypothesis [4]. Study of hemisected implantation sites from murine matings by WM-IHC, which tagged all conceptus-derived cells with GFP, showed that leukocyte interactions with trophoblasts did not occur before gd 9.5 [4]. At gd 9.5, anti-$CD45^+$-stained cell interactions with GFP^+ fetal cells represented $<0.35\%$ of the total visualized $CD45^+$ cell interactions; $CD45^+/CD45^+$ cell pairings were dominant [4, 26]. Because many decidual $CD45^+$ cells are highly proliferative [2, 27, 28] $CD45^+/CD45^+$ cell pairs could represent cell division. However, the first 5 d after implantation is also the time frame when immune interactions can be expected that would result from recognition of posthatching and -implantation conceptus-derived antigens.

Leukocyte activation results from prolonged intervals of contact between cells that form an immunologic synapse [29–31]. Such conjugations, as observed between T cells and APCs or NK cells and their targets, are maintained by cell adhesion molecules that include the LFA (IGTB2, CD11a, formerly LFA-1) and ICAM-1 (CD54). Concentric adhesion rings form at the points of cell contact and give synapses their characteristic flattened appearance [29, 31–35]. Herein, we report our study of $CD45^+$ cell conjugation in live hemisected virgin and gd 3.5–9.5 B6 mouse uteri. Time course, frequency, and identity of $CD45^+$ cells interacting with DBA^- and DBA^+ uNK cell subsets are included.

MATERIALS AND METHODS

Mice

B6 males and females were purchased at 7–10 wk of age from Charles River Laboratories (St.-Constant, QC, Canada). CByJ.B6-Tg(UBC-GFP)30Scha/J (*Gfp*$^{+/-}$) mice, with ubiquitous GFP expression, were purchased from The Jackson Laboratory (Bar Harbor, ME, USA) and bred to be homozygous *Gfp/Gfp* at Queen's University. CByJ.B6-Tg(UBC-GFP)30Scha/J(*Gfp*$^{+/+}$) or B6 males were used as studs to breed B6 females. Matings were timed from copulation plug detection (gd 0.5). Females (virgin or pregnant at gd 3.5, 4.5, 5.5, 6.5, 8.5, or 9.5; n = at least 3 per group) were euthanized by cervical dislocation. Mouse handling was in accordance with the guidelines of the Canadian Council on Animal Care and conducted under animal care protocols approved by Queen's University.

WH-IHC

Implantation sites were studied using WM-IHC as described elsewhere [4]. Any sporadic, abnormally pale, or small implantation sites were excluded from the study. In brief, virgin and gd 3.5–9.5 pregnant uteri were trimmed of mesenteric fat and dissected under microscopic magnification with a scalpel blade. Virgin, and gd 3.5 and 4.5 uteri were bisected at the cervix, and each uterine horn was halved longitudinally along the antimesometrial–mesometrial plane. At gd 5.5, individual implant sites were separated, and each was bisected midsagittally. From gd 6.5 to 9.5, antimesometrial myometrium was incised with fine forceps, retracted from the decidual capsule and trimmed off, leaving a tag of uterine wall for specimen orientation. Then, the decidual capsule and residual mesometrial uterine wall were bisected midsagittally. Samples were incubated in 200 μl PBS-1% BSA-0.1% sodium azide (PBA) for 1 h with 10 μg/ml blocking antibody to the IgG Fc receptor (anti-CD16/CD32; supernatant of hybridoma 2.4G2; American Type Culture Collection, Manassas, VA, USA) and 2–10 μg/ml of up to 3 differently conjugated fluorescent primary antibodies (**Table 1**). For staining with DBA lectin, implantation sites were transferred to 200 μl fresh PBA after the initial 1 h incubation and incubated for a further 10 min with 30 μg/ml FITC- or 15 μg/ml TRITC-conjugated DBA lectin. All antibody combinations are outlined in **Table 2**. Finally, 1 ml PBA was added, and samples were moved onto microscope slides with the cut surface facing upward to expose the embryonic crypt and coverslipped. The slides were viewed by epifluorescence microscopy and photographed with an AxioCam-equipped M1 imager (Zeiss, Toronto, ON, Canada) with Axiovision 4.8 software or a Quorum Wave FX Spinning Disc confocal microscope equipped with Metamorph software (Quorum, Guelph, ON, Canada). Different antibody staining combinations were used to study littermates, except at gd 5.5/6.5, when several implantation sites were needed from each litter to provide a sufficient number of conjugates for analysis.

Conjugate assessment

Epifluorescence images captured at ×200 magnification were analyzed for leukocyte conjugates. Leukocyte–leukocyte pairs were scored as conjugates when 2 $CD45^+$ cells were in close contact, in the same plane of focus, and the cells' membranes were flattened at the point of intercellular contact (**Fig. 1A**). Occasional clusters of $CD45^+$ leukocytes were observed in the decidua basalis but were not counted as conjugates, because the cells comprising them were in different planes of focus and lacked flattened surfaces indicative of cell contact. For pairs scored as conjugates, at least 50 $CD45^+$ cell pairs were counted for each specific antibody combination in uteri (virgin, and gd 3.5–4.5) or implantation sites (gd 5.5–9.5) from 3 different mice. Each cell of a conjugated pair was scored for antibody reactivity. Conjugates were of 2 primary types: homologous conjugates consisting of 2 $CD45^+$ cells that shared expression of the surface marker of interest or heterologous conjugates consisting of 2 $CD45^+$ cells that did not share the surface marker of interest.

Immunohistochemistry

Implantation sites collected from gd 8.5 B6 females (n = 3) were immersion fixed, using 4% PFA, processed, embedded in paraffin, cut into 6 μm sections, and mounted on glass slides. After staining (outlined below), the slides were viewed with an M1 imager and photographed at ×400 magnification with Axiovision 4.8 software (Zeiss).

Dual staining of paraffin-embedded tissue sections with DBA lectin and PAS reagent. Slides were stained for uNK cell subset visualization according to published protocols for DBA lectin and PAS dual staining [12, 18]. Cell phenotypes in the decidua basalis were scored based on PAS reactivity (all uNK cells) and DBA reactivity (unique decidual uNK cells) to identify the PAS^+DBA^- (purple) or PAS^+DBA^+ (brown) uNK cell lineages.

Detection of apoptosis by TUNEL staining. For detection of apoptosis and nuclear fragmentation in implantation sites, TUNEL staining was conducted according to the protocol provided with the TACS2 TdT-DAB In Situ Apoptosis Detection Kit (cat. no. 4810-30 K; Trevigen, Gaithersburg, MD, USA).

Statistical analyses

Statistical significance for conjugated cell counts was assessed by Student's t test or 1-way ANOVA with Tukey's multiple-comparison post hoc test. Significance was set at $P < 0.05$. Data are expressed as means ± SD. Statistical analysis was performed with Prism5 Software (GraphPad Software, Inc.).

TABLE 1. Antibodies used for WM-IHC

Primary antibody	Fluorochrome	Company	Antibody concentration	Working concentration
Anti-mouse CD4	APC	Affymetrix, Santa Clara, CA, USA	0.2 mg/ml	3–4 μg/ml
Anti-mouse CD8a	PE	BioLegend, San Diego, CA, USA	0.2 mg/ml	3–4 μg/ml
Anti-mouse CD8a	APC	BioLegend	0.2 mg/ml	3–4 μg/ml
Anti-mouse CD11c	PE	Affymetrix	0.2 mg/ml	3–4 μg/ml
Anti-mouse CD11a	PE	BioLegend	0.2 mg/ml	3–4 μg/ml
Rat anti-mouse CD31	PE	BD Pharmingen, San Diego, CA, USA	0.2 mg/ml	4 μg/ml
Anti-mouse CD31	FITC	BioLegend	0.5 mg/ml	10 μg/ml
Anti-mouse CD45	APC	BioLegend	0.2 mg/ml	3–4 μg/ml
Anti-mouse CD45	FITC	Affymetrix	0.5 mg/ml	7.5 μg/ml
Anti-mouse CD54	FITC	BioLegend	0.5 mg/ml	7.5 μg/ml
Anti-mouse CD68	PE	BioLegend	0.2 mg/ml	3–4 μg/ml
Anti-mouse Ly49C, Ly49I	PE	BD Pharmingen	0.2 mg/ml	3–4 μg/ml
Anti-mouse MHC II (I-A)	PE	Affymetrix	0.1 mg/ml	2 μg/ml
DBA lectin	FITC	Vector Laboratories, Burlingame, CA, USA	2 mg/ml	30 μg/ml
DBA lectin (horse gram)	TRITC	EY Laboratories, San Mateo, CA, USA	1 mg/ml	15 μg/ml

RESULTS

Assessment of synapse formation in CD45$^+$ leukocyte conjugates within gd 8.5 decidua basalis

In studies with anti-CD45 WM-IHC, CD45$^+$ cells in gd 8.5 decidua basalis of B6 and B6.*Ncr1*$^{Gfp/Gfp}$ mice were shown to pair with other CD45$^+$ cells rather than with trophoblasts [26]. CD45$^+$/CD45$^+$ cell pairs were in the same plane of focus, and each cell was flattened over shared points of contact, which fluoresced more intensely. This appearance (Fig. 1A, B) suggested immunologic synapse formation. To confirm this interpretation, we examined implant sites costained with anti-CD45 APC, anti-CD54 FITC, and anti-CD11a PE antibodies with confocal microscopy. All of the CD45$^+$ cells participating in conjugation expressed either CD54 or CD11a (65% of all conjugates) or expressed both CD54 and CD11a (35% of all conjugates) at the site of cell contact (Fig. 1A). These data indicate that the observed CD45$^+$/CD45$^+$ cell conjugates are adhesion molecule–expressing, immune synapse–coupled cells.

Time course and frequency of CD45$^+$/CD45$^+$ cell conjugates in the decidua basalis

To address when CD45$^+$/CD45$^+$ cell conjugates occur and whether their frequencies are stable, we conducted a time course study in virgin and pregnant mice from gd 3.5 to 9.5. CD45$^+$/CD45$^+$ conjugates were extremely rare in virgin and gd 3.5 and 4.5 uteri (1.4 ± 0.5, 1.5 ± 0.1, and 1.9 ± 0.1%, respectively, of all CD45$^+$ cells counted; at least 500 CD45$^+$ cells scored/uterus), but increased slightly to 3.3 ± 0.8% on gd 5.5, the first day after embryo implantation (Fig. 1C). After implantation, conjugated cells (Fig. 1B) were present only in decidua basalis and were never observed in lateral or antimesometrial decidua. The frequency of CD45$^+$/CD45$^+$ cell conjugates increased significantly from virgin and gd 3.5–5.5 values to 7.8 ± 1.0% by gd 6.5 ($P < 0.001$). The frequency of CD45$^+$/CD45$^+$ conjugates reached its peak at gd 8.5 (19.0 ± 1.8% all CD45$^+$ cells) then fell to 9.8 ± 1.6% by gd 9.5 (Fig. 1C). CD45$^+$ leukocytes increased in diameter across early gestation, regardless of conjugation status. Thus, CD45$^+$/CD45$^+$ leukocyte conjugates present in low numbers in virgin, preimplantation, and peri-implantation uteri, increase significantly in frequency within 24 h of blastocyst implantation and decline in frequency after gd 8.5.

CD31-expressing CD45$^+$ leukocytes are present across early gestation

CD31, an adhesion molecule of the immunoglobulin gene superfamily formerly known as platelet endothelial cell adhesion molecule-1 is expressed by endothelial cells, platelets, and some immune cells [36]. In lymphocytes, CD31 expression is linked to cell activation, inhibition, promotion of transmigration, and angiogenesis [37–39]. Widespread CD31 expression by decidual CD45$^+$ cells is detectable by

TABLE 2. Antibody combinations used in WM-IHC

Antibody 1	Antibody 2	Antibody 3
CD45 APC	DBA FITC	CD8 PE CD11c PE CD31 PE CD68 PE Ly49C/I PE MHCII PE
CD45 APC	Ly49 FITC	CD8 PE CD11c PE CD68 PE MHCII PE
CD45 FITC	CD11c PE	CD8 APC CD4 APC
CD45 FITC	CD4 APC	DBA TRITC Ly49C/I PE
CD45 APC	Ly49C/I PE	CD31 FITC
CD45 APC	CD54 FITC	CD11a PE

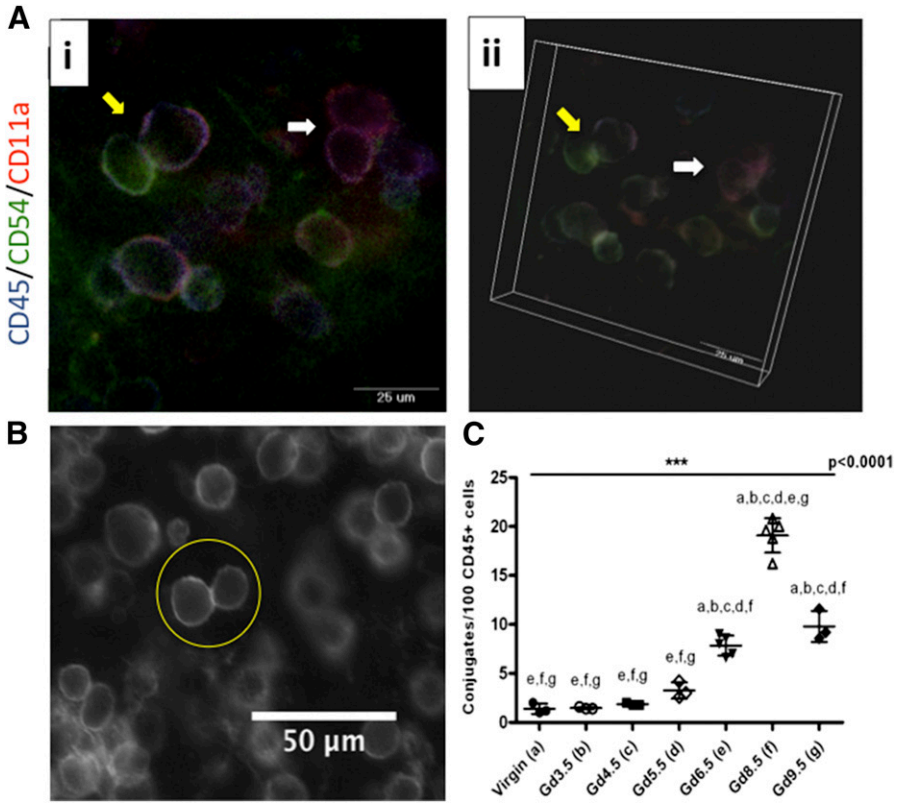

Figure 1. CD45$^+$ cell conjugates and their frequency in C57BL/6 uteri during early pregnancy. (Ai) Confocal microscopy of gd 8.5 B6 decidua stained with anti-CD45 APC (blue), anti-CD54 FITC (green), and anti-CD11a PE (red). Immunologic synapse formation was apparent between CD54$^+$ and CD11a$^+$ leukocytes (CD45$^+$) (yellow arrow). Contacts between CD45$^+$ leukocytes equally reactive for CD11a were considered dividing cells (white arrow). (Aii) Four-dimensional reconstruction of the confocal image in (Ai). CD45$^+$ heterologous conjugates (yellow arrow) and homologous conjugates (white arrow) are indicated. (B) Representative black-and-white WM-IHC of a gd 8.5 implant site stained with anti-CD45 APC. A CD45$^+$ leukocyte conjugate is circled in yellow. (C) Proportions of CD45$^+$ cell conjugates among 100 CD45$^+$ cells at each day studied. Data are means ± SD. One-way ANOVA results are shown at the top of the graph. Letters indicate significance of the Tukey multiple comparison post hoc test between the time points.

WM-IHC and dually expressing CD45$^+$CD31$^+$ cells contribute to conjugates [4, 26]. To determine whether CD31 expression is a prerequisite for decidual CD45$^+$ cell conjugation, implantation sites were costained with anti-CD45 APC and anti-CD31 PE; the latter additionally stained endothelial cells within vessels, which become more complex as gestation progresses. Conjugated and unconjugated decidual leukocytes coexpress CD31$^+$CD45$^+$ on the postimplantation gestation day studied (gd 5.5–9.5) (**Fig. 2A**; Supplemental Fig. 1). When all CD45$^+$ cells were considered, regardless of conjugation status, 47.3 ± 9.1% of gd 5.5 leukocytes coexpressed CD31. Frequencies of CD45 cells coexpressing CD31 increased significantly between gd 5.5 and 6.5 (76.7 ± 5.1%) and remained stable at gd 8.5 (89.3 ± 0.6%) and gd 9.5 (80.7 ± 5.0%; ns; Fig. 2B).

When separated by conjugation status, the proportion of unconjugated CD45$^+$CD31$^+$ cells was stable over early gestation. Over the same interval, proportions of conjugated CD45$^+$CD31$^+$ cells changed (Fig. 2C). Most of these partnerships involved 2 phenotypically identical CD45$^+$CD31$^+$ cells, referred to as homologous conjugates. Fewer conjugates were heterologous (i.e., occurred between a CD45$^+$CD31$^+$ cell and a CD45$^+$CD31$^-$ cell; Fig. 2D). At gd 5.5, 6.0 ± 3.0% of conjugated CD45$^+$ leukocytes involved at least 1 CD45$^+$CD31$^+$ cell. This percentage increased to 29.3 ± 5.8% at gd 6.5, peaked 44.7 ± 7.4% at gd 8.5, and declined to 31.5 ± 11.9% at gd 9.5 (Fig. 2C). Thus, the time course pattern of conjugation for CD45$^+$CD31$^+$ cells resembles that observed for CD45$^+$/CD45$^+$ cell conjugate frequencies (Fig. 1C) and CD31 expression neither prevents nor is necessary for decidual CD45$^+$ cell pairing.

Two distinct uNK cell populations can be defined by WH-IHC in early decidua basalis

To assign lineage relationships among cells participating in conjugate formation and to determine whether these interactions are random, we had to define the frequencies of the most common CD45$^+$ cell lineages in decidua basalis that could be phenotyped by WH-IHC. We expected uNK cells to be the dominant lineage but only had reagents for WM-IHC that identified DBA lectin$^+$ uNK cells, the transplantable uNK cell subset [12]. Studies were first undertaken to identify reagents reactive with the early, abundant PAS$^+$DBA$^-$ uNK cell subset found in histologic sections (**Fig. 3A**). The gd 8.5 implant sites were used because both uNK cell subsets (PAS$^+$DBA$^-$; PAS$^+$DBA$^+$) are found at high abundance in histologic sections at this time. NK1.1, an NK cell marker commonly used for flow cytometry of B6 lineage mice, worked well in WM-IHC, although it is not a useful reagent for staining histologic sections. NK1.1$^+$ reactivity was seen on <1% of DBA$^+$ cells in WM-IHC (Fig. 3B). Ly49C/I, a uNK cell receptor classified as having inhibitory activity, was also nonreactive on DBA$^+$ uNK cells. Triple staining with DBA and both of these possible DBA$^-$ uNK cell markers revealed that, of DBA$^-$ cells, 72% dually expressed NK1.1 and Ly49C/I (Fig. 3B). Minor DBA$^-$ uNK cell subsets were also observed that exclusively expressed either NK1.1 or Ly49C/I. Although either marker seemed suitable for identification of the DBA$^-$ uNK cell subset using WM-IHC, anti-Ly49C/I was chosen because background

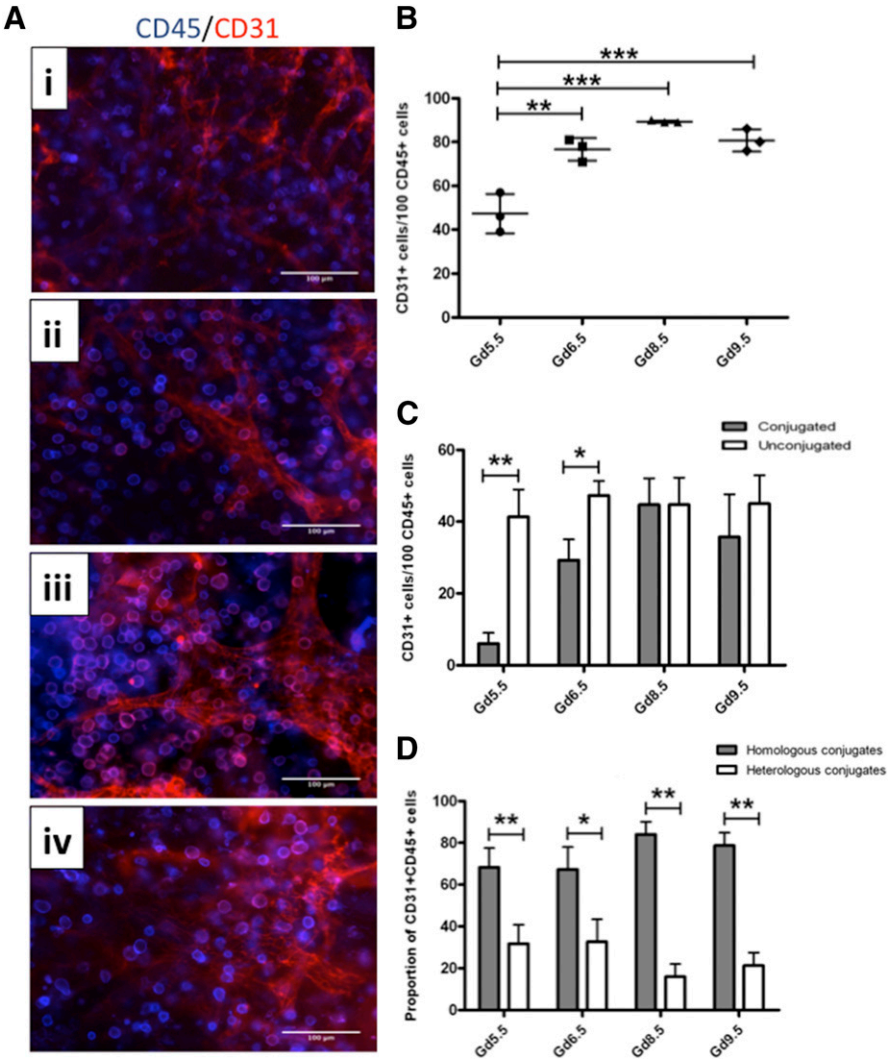

Figure 2. CD45$^+$ cells coexpress CD31 from gd 5.5 to 9.5 in C57BL/6 implantation sites. (A) WM-IHC of B6 implantation sites costained with anti-CD45 APC (blue) and anti-CD31 PE (red). CD31 expression was prevalent on both endothelial cells and CD45$^+$ leukocytes at gd 5.5 (Ai), 6.5 (Aii), 8.5 (Aiii), and 9.5 (Aiv). Blood vessels became more complex, and coexpression of CD31 by CD45$^+$ leukocytes increased as gestation progressed. (B) Proportion of CD45$^+$ leukocytes coexpressing CD31 among 100 CD45$^+$ leukocytes. Coexpression increased from gd 5.5 to 6.5 and then remained stable. (C) CD31$^+$ expression by CD45$^+$ leukocytes differs between conjugated and unconjugated cells at gd 5.5 and 6.5. (D) Within the population of conjugated CD45$^+$ leukocytes that coexpressed CD31, most represented homologous conjugation of 2 CD31$^+$CD45$^+$ cells. Heterologous conjugates of 1 CD31$^+$CD45$^+$ and 1 CD31$^-$CD45$^+$ cell are less common across early gestation. Data are means ± SD. $*P < 0.05$, $**P < 0.01$, $***P < 0.001$.

fluorescence was much lower than when anti-NK1.1 was used (unpublished observations).

Ly49C/I$^+$ uNK cells were present at a stable frequency before conception (virgin: 10.7 ± 1.5%) and throughout the peri-implantation period (gd 3.5: 12.0 ± 1.7%; gd 4.5: 13.7 ± 3.2%). The DBA$^+$ subset was absent at these times. DBA$^+$ uNK cells appeared in the decidua basalis on gd 5.5, but were less frequently present than Ly49C/I$^+$ cells (7.0 ± 1.7% vs. 23.7 ± 1.5% of total CD45$^+$ cells; $P < 0.001$). Ly49C/I$^+$ cells increased significantly in frequency between gd 4.5 and 5.5 ($P = 0.008$). By gd 6.5, the frequencies of both Ly49C/I$^+$ cells and DBA$^+$ cells had increased within decidua basalis with Ly49C/I$^+$ cells remaining statistically dominant (Ly49C/I$^+$: 32.7 ± 3.1% vs. DBA$^+$: 17.0 ± 3.4%; $P = 0.001$). By gd 8.5, DBA$^+$ uNK cells represented half of all CD45$^+$ decidual cells (49.0 ± 8.7%), whereas Ly49C/I$^+$ uNK cell frequency was 20.3 ± 3.5%, a statistically significant drop from gd 6.5 ($P = 0.01$). At gd 9.5 DBA$^+$ uNK cell frequency remained higher than Ly49C/I$^+$ uNK cell frequency (43.5 ± 6.2% vs. 20.5 ± 5.0%, respectively; $P = 0.005$) (Fig. 3C). Thus, Ly49C/I$^+$ cells in WM-IHC showed the same dynamic pattern as that reported for PAS$^+$DBA$^-$ uNK cells in tissue sections [12] and is the dominant NK cell subset in decidua basalis up to gd 8.5. At gd 8.5, summation of cells expressing Ly49C/I or DBA provides a uNK cell estimate of ~70% of all CD45$^+$ decidual cells, a value similar to that reported for early human decidua.

Conjugate formation by Ly49C/I$^+$ and DBA$^+$ uNK cell subsets

PAS$^+$ DBA$^-$ and PAS$^+$ DBA$^+$ uNK cells have been identified in very close proximity in PAS and DBA dually stained tissue sections from early mouse implant sites (Fig. 3A), but this method is inferior to live cell WH-IHC for recognition and quantification of conjugated cell pairs (Fig. 3D). Thus, the frequency of conjugates involving Ly49C/I$^+$ or DBA$^+$ uNK cells was addressed by WM-IHC. Ly49C/I$^+$/Ly49C/I$^+$ homologous conjugates, which could represent dividing cells, were present in a small number in virgin (2.2 ± 1.9% of all CD45$^+$ cell conjugates) and in gd 3.5 (2.2 ± 3.8%) uteri (**Fig. 4A**). These conjugates increased nonsignificantly to gd 4.5 (5.6 ± 1.9%) and gd 5.5 (10.0 ± 2.0%) and then rose significantly to peak at gd 6.5 (16.6 ± 8.4% of all CD45$^+$ cell conjugates). After this time, Ly49C/I$^+$ homologous conjugates declined significantly to

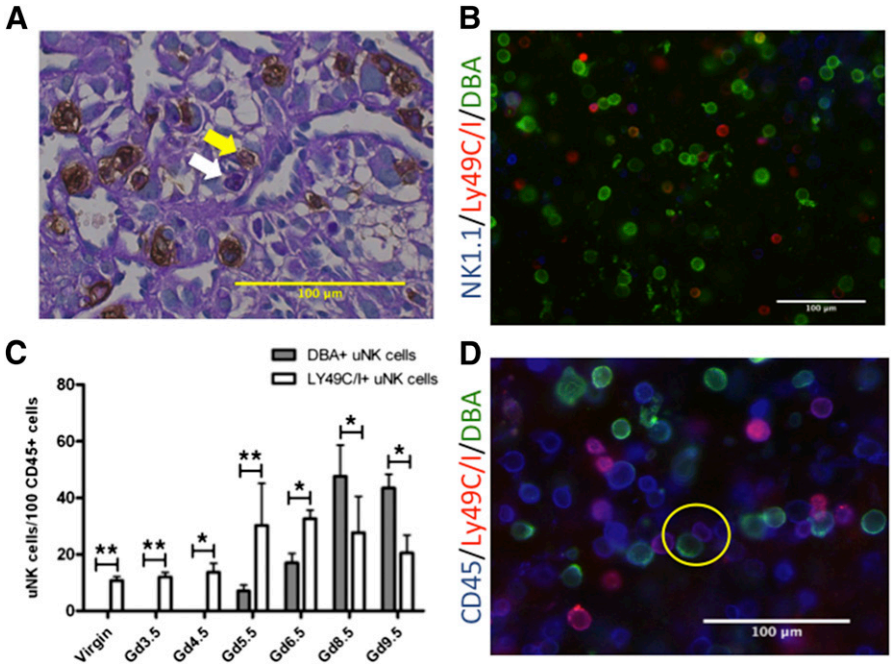

Figure 3. Detection and frequencies of 2 uNK cell subsets in early C57BL/6 decidua basalis. (A) DBA/PAS dual staining of paraffin-embedded sections show PAS^+DBA^- (purple, white arrow) and PAS^+DBA^+ (brown, yellow arrow) uNK cells in close proximity. (B) WM-IHC triple staining with anti-NK1.1 APC (blue), anti-Ly49C/I PE (red), and DBA lectin FITC (green). Little overlap was observed between anti-NK1.1 or anti-Ly49C/I and DBA lectin expression. $Ly49C/I^+$ cells represent the DBA^- subset of uNK cells. (C) Examination of Ly49C/I and DBA lectin expression by $CD45^+$ leukocytes. $Ly49C/I^+$ uNK cells were dominant before implantation and early in gestation (gd 5.5 and 6.5). DBA^+ uNK cells were not present before implantation but overtook $Ly49C/I^+$ uNK cells in frequency at gd 8.5. Data are means ± SD. $*P < 0.01$, $**P < 0.001$. (D) WM-IHC of anti-CD45 APC (blue), anti-Ly49 PE (red), and DBA lectin FITC (green) revealed conjugate formation between $Ly49C/I^+$ and DBA^+ uNK cells (circled in yellow).

peri-implantation levels at gd 8.5 (4.0 ± 3.3%) and gd 9.5 (4.0 ± 0.0%). $Ly49C/I^+$ uNK cells also conjugated with $CD45^+$ cells that were nonreactive for $Ly49C/I^+$ (heterologous conjugates). $Ly49C/I^+$ heterologous conjugates represented 15.6 ± 5.1% of all $CD45^+$ cell conjugates in the virgin uterus and 21.1 ± 5.1% of cell conjugates at gd 3.5 (Fig. 4B). The number of $Ly49C/I^+$ heterologous conjugates rose significantly at gd 4.5 (34.4 ± 6.9%) and remained constant at gd 5.5 (26.0 ± 3.5%) and gd 6.5 (34.7 ± 4.2%), before declining at gd 8.5 (20.0 ± 3.3%; $P < 0.001$ vs. gd 6.5) and gd 9.5 (18.7 ± 1.2%; $P = 0.003$ vs. gd 6.5, $P = 0.537$ vs. gd 8.5).

DBA^+ uNK cells were absent in virgin and gd 3.5and 4.5 uteri (Figs. 3C, 4C, 4D). At gd 5.5, DBA^+ uNK cells were found in 6.0 ± 2.8% of all $CD45^+/CD45^+$ cell pairs, but were never observed as

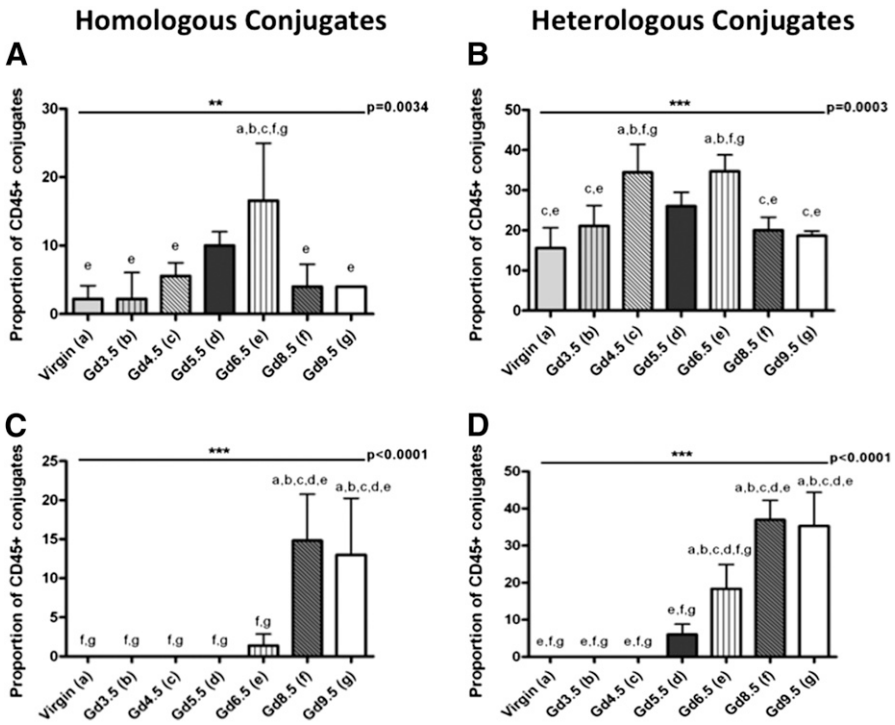

Figure 4. UNK cell subsets contribute to $CD45^+$ leukocyte conjugates in early C57BL/6 decidua basalis. (A) $Ly49C/I^+$ uNK cells in homologous conjugates in virgin and gd 3.5–9.5 uteri. (B) $Ly49C/I^+$ uNK cells in heterologous conjugates in virgin and gd 3.5–9.5 uteri. (C, D) DBA^+ uNK cells were not present in preimplantation uteri but were common in homologous conjugates (C) at gd 8.5 and 9.5. (D) DBA^+ uNK cell heterologous conjugates were initiated at gd 5.5 and increased from gd 6.5 to 8.5 as the number of DBA^+ uNK cells increased. Data are means ± SD. One-way ANOVA results are shown at the top of each graph. Letters indicate significance of Tukey's multiple comparison post hoc test between the time points.

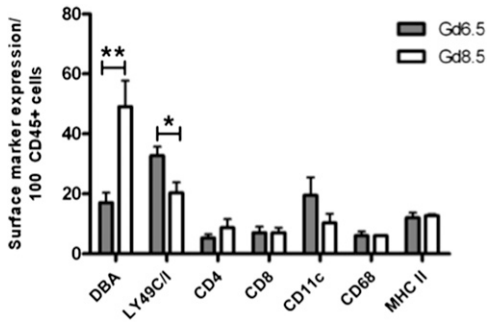

Figure 5. Leukocyte lineages other than uNK cells are constant from gd 6.5 to 8.5. Expression of leukocyte markers by $CD45^+$ cells at gd 6.5 and 8.5. Ly49C/I^+ leukocytes decreased from gd 6.5 to 8.5, whereas DBA^+ leukocytes increased in number between these 2 time points. All other leukocyte lineages remained unchanged from gd 6.5 to 8.5. Data are means ± SD. *$P < 0.05$, **$P < 0.001$.

DBA^+/DBA^+ homologous conjugates (Fig. 4C, D), suggesting that DBA^+ cells had migrated into or differentiated within the uterus, but cell division had not commenced. By gd 6.5, DBA^+/DBA^+ homologous conjugates represented 1.4 ± 1.5% of all $CD45^+$ cell conjugates, whereas heterologous DBA^+CD45^+/DBA^-CD45^+ conjugates represented 18.3 ± 6.6%. Between gd 6.5 and 8.5, DBA^+/DBA^+ homologous conjugates increased to 14.8 ± 5.9% ($P < 0.001$ vs. gd 6.5), whereas DBA^+ heterologous conjugates increased to 36.9 ± 5.2% ($P < 0.001$ vs. gd 6.5). DBA^+ uNK cells were therefore incorporated into more than half of all gd 8.5 $CD45^+$ cell conjugates, and this frequency was similar at 9.5 (homologous: 13.0 ± 7.2%, $P = 0.541$; 35.3 ± 9.0%, $P = 0.596$ vs. gd 8.5).

Composition of uNK cell conjugates at gd 6.5 and 8.5

Because heterologous conjugates containing a single Ly49I/C^+ uNK cell or a single DBA^+ uNK cell are relatively abundant at gd 6.5 and 8.5, these time points were studied further to identify the $CD45^+$ partners of uNK cells. Preliminary studies defined the frequencies of 5 leukocyte lineages detectable by WM-IHC (**Fig. 5**). APCs reactive with MHCII antibodies were constant in frequency between gd 6.5 (12.0 ± 1.7%) and 8.5 (12.7 ± 0.6%; $P = 0.561$), as were the frequencies of $CD68^+$ decidual macrophages (6.0 ± 1.4% at gd 6.5 and 6.0 ± 0.0% at gd 8.5; $P = 0.99$). A third group of potential APCs, $CD11c^+$ DCs, appeared to decrease between gd 6.5 (19.5 ± 6.0%) and 8.5 (10.3 ± 3.1%), but the decrease was not statistically significant ($P = 0.062$). T lineage cells were less frequent than APCs, with $CD8^+$ cells accounting for 7.0 ± 2.0% and 7.0 ± 1.7% of all $CD45^+$ cells at gd 6.5 and 8.5, respectively ($P = 0.99$). $CD4^+$ T cells represented 5.3 ± 1.2% of $CD45^+$ cells at gd 6.5 and 8.7 ± 2.9% at gd 8.5 ($P = 0.137$). Thus, with the exception of Ly49C/I^+ and DBA^+ uNK cells, major $CD45^+$ decidual leukocyte populations appear to be stable between gd 6.5 and 8.5 (Fig. 5).

Heterologous conjugation of cells expressing one of the 5 surface markers with either Ly49C/I^+ or DBA^+ uNK cells was assessed in samples costained for anti-CD45, anti-Ly49C/I, or DBA lectin and a third reagent (Table 2; **Fig. 6**). The 2 uNK cell subtypes were primary partners for each other in heterologous conjugates, with 1 cell identified as either Ly49C/I^+ or DBA^+ (Figs. 3D, **7**). Ly49C/I^+/DBA^+ pairs formed 26.7 ± 11.5% of heterologous uNK cell conjugates at gd 6.5 (Fig. 7A). At gd 6.5 Ly49C/I^+ or DBA^+ uNK cells were conjugated with $MHCII^+$ cells (19.0 ± 12.3% and 13.5 ± 18.0%, respectively), $CD11c^+$ DCs (26.8 ± 7.8% and 14.4 ± 18.1%, respectively), and $CD68^+$ decidual macrophages (10.7 ± 2.5% and 12.3 ± 10.3%, respectively) (Figs. 6A–C, 7A). Conjugation with $CD8^+$ cells was more limited for both Ly49C/I^+ (4.7 ± 4.2%) and DBA^+ (3.7 ± 6.4%) uNK cells. No conjugates were detected with $CD4^+$ T cells for either uNK cell subset at gd 6.5 (Fig. 7A) (CD3 is not an effective reagent in mouse decidual WM-IHC.) There were no significant differences between Ly49C/I^+ or DBA^+ uNK cells in the frequencies of different heterologous conjugates formed at gd 6.5 (Fig. 7A).

At gd 8.5, conjugations between the 2 uNK cell subsets represented 24.9 ± 6.7% of all heterologous uNK cell conjugates (Fig. 7B). This frequency was not significantly different from that

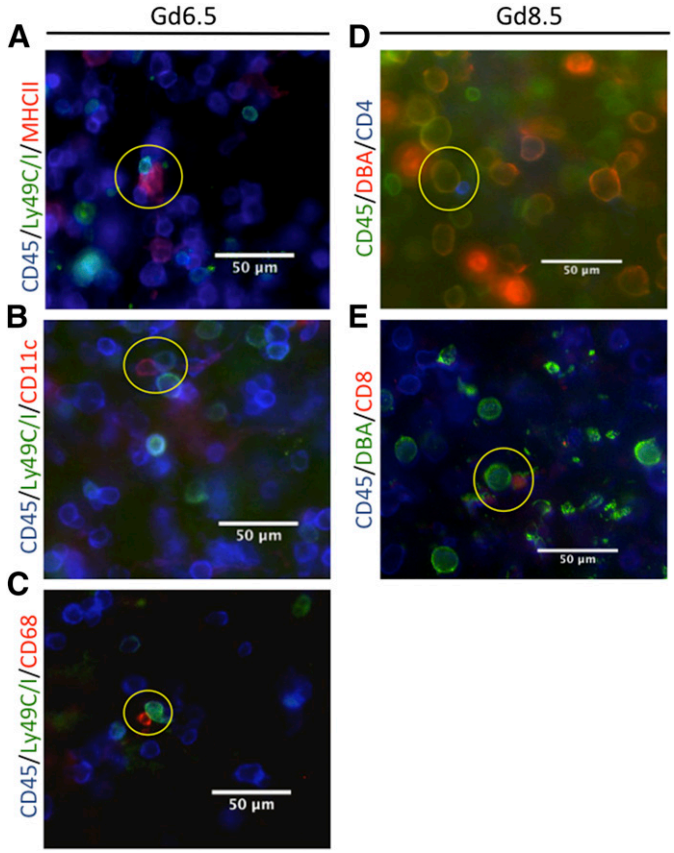

Figure 6. Leukocytes are observed in conjugates with uNK cells at gd 6.5 and 8.5. (A–C) WM-IHC images of heterologous conjugates with Ly49C/I^+ uNK cells at gd 6.5. Implant sites were stained with anti-CD45 APC (blue), anti-Ly49C/I FITC (green) and (A) anti-MHCII PE (red), (B) anti-CD11c PE (red), or (C) anti-CD68 PE (red). Conjugations between Ly49C/I^+ uNK cells and APCs are circled in yellow. (D, E) WM-IHC images of heterologous conjugates with DBA^+ uNK cells at gd 8.5. Implant sites were stained with (D) anti-CD45 FITC (green), DBA lectin TRITC (red), and anti-CD4 APC (blue), or (E) anti-CD45 APC (blue), DBA lectin FITC (green), and anti-CD8 PE (red). Yellow circles: conjugations between DBA^+ uNK cells and T cells.

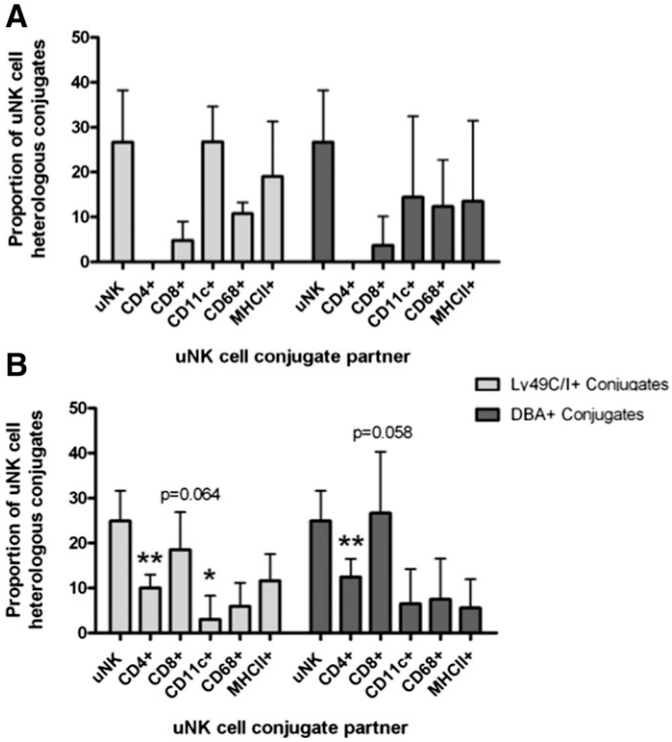

Figure 7. Proportion of leukocytes forming conjugates with uNK cells at gd 6.5 and 8.5. (A) At gd 6.5, conjugations between Ly49C/I$^+$ and DBA$^+$ uNK cell subsets accounted for 26.7% of CD45$^+$ heterologous conjugates. APCs (CD11c$^+$, CD68$^+$, and MHCII$^+$) were the dominant CD45$^+$ cell populations found in conjugation with Ly49C/I$^+$ (pale gray) and DBA$^+$ (dark gray) uNK cells at gd 6.5. CD8 T cells represent a smaller population of heterologous conjugates, and no conjugations were observed between CD4$^+$ T cells and either uNK cell subset. (B) At gd 8.5, conjugations between Ly49C/I$^+$ and DBA$^+$ uNK cell subsets account for 24.9% of heterologous conjugates. T cells (CD4$^+$, CD8$^+$), are the dominant populations found in conjugation with Ly49C/I$^+$ (light gray) and DBA$^+$ (dark gray) uNK cells at gd 8.5. Conjugations still occurred with APCs (CD11c$^+$, CD68$^+$,and MHCII$^+$), but to a lesser extent than at gd 6.5. There was no significant difference in conjugate composition between the 2 uNK cell subsets at gd 6.5 or 8.5. Data are means ± SD. *$P < 0.05$, **$P < 0.01$ vs. gd 6.5.

of these interactions at gd 6.5 ($P = 0.808$), despite the significant increase in the DBA$^+$ uNK cell population between these 2 time points. Although frequencies of CD45$^+$ leukocytes phenotypically classified as non-uNK cells were stable between gd 6.5 and 8.5, contributions of these lineages to Ly49C/I$^+$/CD45$^+$ or DBA$^+$/CD45$^+$ heterologous conjugates changed dramatically between gd 6.5 and 8.5. At gd 8.5, fewer pairings were observed with potential APCs, and more were seen with T cells, including for the first-time conjugates that involved CD4 T cells (Figs. 6D, E, 7B). At gd 8.5, frequencies of Ly49C/I$^+$ and DBA$^+$ uNK cells conjugated with MHCII$^+$ cells were 11.5 ± 5.9% ($P = 0.401$ vs. gd 6.5) and 5.6 ± 6.4% ($P = 0.507$ vs. gd 6.5), respectively. Similar Ly49C/I$^+$ and DBA$^+$ conjugations with CD11c$^+$ cells were 3.3 ± 5.2% ($P = 0.012$ vs. gd 6.5) and 6.5 ± 7.7% ($P = 0.452$ vs. gd 6.5), respectively, and those with CD68$^+$ cells were 5.9 ± 5.2% ($P = 0.223$ vs. gd 6.5) and 7.5 ± 9.0% ($P = 0.508$ vs. gd 6.5), respectively (Fig. 7B). At gd 8.5, CD8$^+$ T cells were present in 18.5 ± 8.3% of Ly49C/I$^+$/CD45$^+$ conjugates ($P = 0.064$ vs. gd 6.5) and 26.7 ± 13.7% of DBA$^+$CD45$^+$ conjugates ($P = 0.058$ vs. gd 6.5) (Figs. 6E, 7B). CD4$^+$ T cells were partners in 10.0 ± 2.9% of Ly49C/I$^+$ conjugates ($P = 0.004$ vs. gd 6.5) and 12.5 ± 4.0% of DBA$^+$ conjugates ($P = 0.006$ vs. gd 6.5) (Fig. 7B). TUNEL staining of tissue sections from gd 8.5 implantation sites revealed no evidence of apoptosis in stromal cells or leukocytes within the decidua basalis (Supplemental Fig. 2), suggesting that heterologous leukocyte conjugations in the early decidua do not result in cell death.

gd 6.5 and 8.5 CD45$^+$ cell conjugates independent of uNK cells

As suggested by the stability of other phenotyped leukocyte lineages within gd 6.5 and 8.5 decidua (Fig. 5), no homologous conjugates (putative proliferating cells) were observed between CD4$^+$, CD8$^+$, and CD68$^+$ cells at gd 6.5. MHCII$^+$ and CD11c$^+$ homologous conjugates were present at low frequencies (0.5 ± 1.0% and 0.7 ± 1.2%, respectively). At gd 8.5, CD8$^+$ and CD68$^+$ homologous conjugates were still absent, MHCII$^+$ homologous conjugates remained low (0.5 ± 0.9%), and CD11c$^+$ homologous conjugate frequency was 2.0 ± 2.0% ($P = 0.374$ vs. gd 6.5). CD4$^+$ homologous conjugates appeared at a frequency of 0.7 ± 1.2% of all CD45$^+$ conjugates accounting for the slight but nonsignificant increase in CD4$^+$ leukocytes between gd 6.5 and 8.5.

The cell lineages investigated in this study also participated in heterologous CD45$^+$ conjugations that did not involve uNK cells (Supplemental Fig. 3A–D). Analyses of these uNK cell-independent heterologous conjugates focused on T cell interactions with CD11c$^+$ DCs. Although some murine decidual DCs express CD8a [40–42], coexpression of the 2 markers had a frequency of <1% in our WM-IHC, permitting analyses using costaining with anti-CD45 FITC, anti-CD11c PE, and either anti-CD4 (Supplemental Fig. 3E) or anti-CD8 APC antibodies (Supplemental Fig. 3F). No conjugations were observed between CD11c$^+$ DCs and either T cell subset at gd 6.5 (Supplemental Fig. 3E, F) or 8.5. Thus, although heterologous conjugates not involving uNK cells are frequent between CD45$^+$ decidual leukocytes, these conjugates are not between T cells and CD11c$^+$ DCs. Because of the low frequencies of CD4$^+$ cell homologous and heterologous conjugates and of Foxp3 expressing cells at these time points (2.5–3.2% by FACS; data not shown), the participation of regulatory T cells in conjugate formation could not be estimated.

DISCUSSION

The goal of this study was to determine the frequency, time course, and composition of leukocyte conjugates in early mouse decidua. Although CD45$^+$ leukocytes are present in the uterus before implantation and throughout early decidua, conjugated cell pairs appear only in decidua basalis, the site of leukocyte enrichment, during early to midpregnancy in mice. WM-IHC provides a more sensitive method for conjugate visualization than IHC studies of paraffin-embedded sections that cannot confirm direct leukocyte–leukocyte contact [43], because of the possible transient nature of such conjugates [35]. Leukocyte conjugates were present infrequently in the pre- and peri-implantation

period and increased within 1 day of blastocyst implantation (gd 4.0–4.5) [44], reaching peak numbers at gd 8.5. Phenotypes of conjugated leukocyte pairs were complex, but almost all conjugates included at least 1 cell, and most had 2 cells, with high expression of CD31. Acquisition of the $CD31^{high}$ phenotype by $CD45^+$ cells is reported in T, B, and NK cells as well as in granulocytes, dendritic cells, and macrophages [45–49], and reflects activation and regulation of leukocyte immune responses [36, 45, 46, 49]. Dual staining with anti-CD31 and either anti-Ly49C/I or DBA lectin, confirmed that uNK cells expressed high levels of surface CD31. Many $CD31^+$ decidual leukocytes remained as singlets, which suggests that cell activation occurs independent of synapse formation and that CD31 expression is not necessary for conjugate formation. Rather, acquisition of CD31 appears to reflect broad changes across the entire $CD45^+$ cell population shortly after implantation and may represent endocrine or stromal influences.

The assessment of $CD45^+$ leukocyte phenotypes by WM-IHC identified the majority (at least to 70%) of decidual leukocytes as uNK cells reactive to Ly49C/I or DBA lectin [17, 18]. These findings are consistent with data from previous FACS analyses [4] and IHC studies [50]. Both uNK cell lineages appeared to be highly proliferative, as assessed by the presence of homologous conjugates, which were rare in the other leukocyte lineages analyzed. The other leukocyte lineages had frequencies that were stable between gd 6.5 and 8.5 and at levels similar to those previously reported using other techniques. APCs, including DCs and macrophages, were the second most populous leukocytes [4, 5, 51], whereas T cell frequencies were low [8, 9].

Throughout early gestation, conjugations were observed between $Ly49C/I^+$ and DBA^+ uNK cells. Both uNK cell subsets were present in the uterus from gd 5.5 to 12.5 and had relatively similar distribution patterns [12]. Indeed, DBA^- and DBA^+ uNK cells frequently resided adjacent to each another in histologic sections of the decidua basalis (Fig. 4) [12], although this proximity was not observed within the mesometrial lymphoid aggregate of pregnancy. Heterologous uNK–uNK cell conjugates may represent important intralineage interactions between gd 6.5 and 8.5, because they are sustained as uNK cell subset dominance shifts and they are equivalent or greater in frequency than the interactions with any other leukocyte lineage. ILCs are currently undergoing intensive reclassification studies. Not only are tissue resident NK cells recognized as distinct from conventional NK cells in many tissues, including virgin uterus [13], but ILCs have been transcriptionally separated into ILC-1, -2, or -3 [52]. The position of uNK cells within this newer classification system is not yet fully understood, and it remains possible that DBA^- and DBA^+ uNK cells are distinct cell lineages [53] whose conjugation may be regulatory or stimulatory. An alternate hypothesis is that division of DBA^- uNK cells gives rise to DBA^+ uNK cell progeny. Absence of established methods to support mouse uNK cell proliferation in culture makes the latter hypothesis difficult to assess at present.

APCs of the DCs or macrophage lineage appeared to be the primary partners of both $Ly49C/I^+$ and DBA^+ uNK cells in early gd 6.5 mouse decidua basalis. In late $CD11c^+$ lineage development, certain cells gain CD8α expression. $CD8\alpha^+$ DCs (lymphoid lineage) help direct the development of Th1 type $CD4^+$ helper T cell responses and promote cytotoxic T cell responses from $CD8^+$ T cells [40]. Conversely, the $CD8\alpha^-$ myeloid lineage DCs drive Th2 type $CD4^+$ T cell responses. A study of mouse decidual DCs between gd 1.5 and 17.5 reported a low number of $CD11c^+CD8\alpha^+$ DCs with a peak frequency occurring at gd 5.5. A much higher number of $CD11c^+CD8\alpha^-$ DCs were present across this time [51]. We found a virtual absence of $CD11c^+CD8\alpha^+$ DCs in early decidua and conclude that uNK cells conjugate with myeloid DCs. Interactions between decidual NK cells and DCs have been observed somewhat later in mouse and human pregnancies [43, 54–58] and they are seen in other organs [59], where a variety of outcomes are described. Because no decidual cell death could be detected in the decidua basalis, early decidual DC–NK cell interactions are more likely to result in cytokine production, for example *trans*-presentation of IL15, which may drive either uNK cell proliferation [60] or DC maturation [61]. Contact interactions mediated by receptor–ligand interactions are also recognized between monocytes/macrophages and NK cells, often in the context of enhancing NK cell responses to tumors or microbial pathogens [62]. Interactions between these lineages have not been well studied in either mouse or human decidua, but it is postulated that they dampen uNK cell cytotoxicity [55, 56, 63]. The recent documentation of trogocytosis by human uNK cells [64] enlarges the scope of potential outcomes for uNK cells that may result from interactions with other cell types. Published evidence also supports that uNK/DC interactions are regulatory for other cell lineages including T cells [65, 66].

By gd 8.5, uNK cell partners in conjugates shift away from APCs toward T cells. This timing is inconsistent with a role for T cell conjugation in either activation or deactivation of uNK cells, since uNK cells express CD31 by gd 6.5 and do not show degenerative signs until gd 12.5 [50]. Many model systems, however, show cross-regulatory activities between NK cells and T cells. For example, activated NK cells limit T cell expansion after hematopoietic stem cell transplantation by cytokine-based rather than lytic mechanisms [67–69]. Also, NK cell–T cell interactions are often addressed in the context of microbial infections or carcinogenesis, where NK-cell-mediated killing of activated $CD4^+$ or $CD8^+$ T cells is reported and associated with transient T cell acquisition of NK cell targets during the activation process [70, 71]. Reciprocally, $CD4^+CD25^+$ T-regulatory cells suppress NK cell functions [72, 73]. The absence of detectable cell death in the decidua basalis (Supplemental Fig. 2) is consistent with studies in humans, which found that uNK cells lack the ability to polarize perforin granules to their surfaces [74] and suggests different outcomes for NK cell–T cell interactions. Regulation of T cell activity is considered essential for promotion of fetal tolerance [9, 58]. Our data, however, suggest that neither $CD8^+$ nor $CD4^+$ T cells are primed by APCs, particularly $CD11c^+$ DCs, in the early decidua basalis, because no conjugations are detectable between these lineages, at least from gd 6.5 to 8.5, when the maximum number of immune synapses are found. Although uterine draining lymph nodes are sites in which paternal antigen presentation occurs [42], conjugation of T cells by decidual $CD45^+$ cells may have distinctly different physiologic roles. One role that should be considered is in the modulation of blood pressure, which declines in mice from

gd 5.5 to 9.5 and then rebounds to baseline [75]. Key roles for several CD45$^+$ cell lineages are described in vascular regulation, with regulatory bypass culminating in hypertension.

The decidual leukocyte interactions described in this study reflect events occurring immediately after blastocyst implantation. This time of initial decidual differentiation and maturation is not generally accessible for study in humans and its complexity is not yet captured in decidua culture systems [76, 77]. Multiple lineages of CD45$^+$ cells appear to interact with each another and with blood vessels [4] before significant trophoblast invasion into the decidua basalis. The outcomes from these interactions and their importance for optimizing placental bed development to support pregnancy are important areas for continued study.

AUTHORSHIP

A.M.F. conducted all experiments, analyzed all of the data, prepared the figure plates, and wrote the manuscript. B.A.C. designed the experiments, reviewed all of the data, and contributed to preparation and editing of the manuscript.

ACKNOWLEDGMENTS

This study was supported by Natural Sciences and Engineering and Research Council, Innovation Canada, and the Canadian Research Council program. The authors thank Dr. Patricia Lima, Ottawa for sharing her initial observations regarding the specificity of LY49C/I in WM-IHC and Andra Banete, Mackenzie Redhead, and Matt Gordon of Queen's University for helpful discussions and technical assistance.

DISCLOSURES

The authors declare no conflicts of interest.

REFERENCES

1. Peel, S., Stewart, I. (1988) Time course of the differentiation of granulated metrial gland cells in chimeric mice. *Cell Differ. Dev.* **25,** 197–202.
2. Peel, S. (1989) Granulated metrial gland cells. *Adv. Anat. Embryol. Cell Biol.* **115,** 1–112.
3. Lash, G. E., Otun, H. A., Innes, B. A., Percival, K., Searle, R. F., Robson, S. C., Bulmer, J. N. (2010) Regulation of extravillous trophoblast invasion by uterine natural killer cells is dependent on gestational age. *Hum. Reprod.* **25,** 1137–1145.
4. Croy B.A., Chen Z., Hofmann A.P., Lord E.M., Sedlacek A.L., Gerber S.A. (2012) Imaging of vascular development in early mouse decidua and its association with leukocytes and trophoblasts. *Biol. Reprod.* **87,** 125.
5. Wang, B., Koga, K., Osuga, Y., Cardenas, I., Izumi, G., Takamura, M., Hirata, T., Yoshino, O., Hirota, Y., Harada, M., Mor, G., Taketani, Y. (2011) Toll-like receptor-3 ligation-induced indoleamine 2, 3-dioxygenase expression in human trophoblasts. *Endocrinology* **152,** 4984–4992.
6. Plaks, V., Birnberg, T., Berkutzki, T., Sela, S., BenYashar, A., Kalchenko, V., Mor, G., Keshet, E., Dekel, N., Neeman, M., Jung, S. (2008) Uterine DCs are crucial for decidua formation during embryo implantation in mice. *J. Clin. Invest.* **118,** 3954–3965.
7. Blois, S. M., Klapp, B. F., Barrientos, G. (2011) Decidualization and angiogenesis in early pregnancy: unravelling the functions of DC and NK cells. *J. Reprod. Immunol.* **88,** 86–92.
8. Erlebacher, A. (2013) Immunology of the maternal-fetal interface. *Annu. Rev. Immunol.* **31,** 387–411.
9. Nancy, P., Erlebacher, A. (2014) T cell behavior at the maternal-fetal interface. *Int. J. Dev. Biol.* **58,** 189–198, 189–198.
10. Chen Z., Zhang J., Hatta K., Lima P.D., Yadi H., Colucci F., et al (2012) DBA-Lectin reactivity defines mouse uterine natural killer cell subsets with biased gene expression. *Biol. Reprod.* **87,** 81.
11. Yadi, H., Burke, S., Madeja, Z., Hemberger, M., Moffett, A., Colucci, F. (2008) Unique receptor repertoire in mouse uterine NK cells. *J. Immunol.* **181,** 6140–6147.
12. Zhang, J. H., Yamada, A. T., Croy, B. A. (2009) DBA-lectin reactivity defines natural killer cells that have homed to mouse decidua. *Placenta* **30,** 968–973.
13. Sojka, D. K., Plougastel-Douglas, B., Yang, L., Pak-Wittel, M. A., Artyomov, M. N., Ivanova, Y., Zhong, C., Chase, J. M., Rothman, P. B., Yu, J., Riley, J. K., Zhu, J., Tian, Z., Yokoyama, W. M. (2014) Tissue-resident natural killer (NK) cells are cell lineages distinct from thymic and conventional splenic NK cells. *eLife* **3,** e01659.
14. Degaki, K. Y., Chen, Z., Yamada, A. T., Croy, B. A. (2012) Delta-like ligand (DLL)1 expression in early mouse decidua and its localization to uterine natural killer cells. *PLoS One* **7,** e52037.
15. Hofmann, A. P., Gerber, S. A., Croy, B. A. (2014) Uterine natural killer cells pace early development of mouse decidua basalis. *Mol. Hum. Reprod.* **20,** 66–76.
16. Zhang, J., Dunk, C. E., Lye, S. J. (2013) Sphingosine signalling regulates decidual NK cell angiogenic phenotype and trophoblast migration. *Hum. Reprod.* **28,** 3026–3037.
17. Bianco, J., Stephenson, K., Yamada, A. T., Croy, B. A. (2008) Time-course analyses addressing the acquisition of DBA lectin reactivity in mouse lymphoid organs and uterus during the first week of pregnancy. *Placenta* **29,** 1009–1015.
18. Paffaro, V. A., Jr., Bizinotto, M. C., Joazeiro, P. P., Yamada, A. T. (2003) Subset classification of mouse uterine natural killer cells by DBA lectin reactivity. *Placenta* **24,** 479–488.
19. Chiossone, L., Vacca, P., Orecchia, P., Croxatto, D., Damonte, P., Astigiano, S., Barbieri, O., Bottino, C., Moretta, L., Mingari, M. C. (2014) In vivo generation of decidual natural killer cells from resident hematopoietic progenitors. *Haematologica* **99,** 448–457.
20. Ashkar, A. A., Di Santo, J. P., Croy, B. A. (2000) Interferon gamma contributes to initiation of uterine vascular modification, decidual integrity, and uterine natural killer cell maturation during normal murine pregnancy. *J. Exp. Med.* **192,** 259–270.
21. Charalambous, F., Elia, A., Georgiades, P. (2012) Decidual spiral artery remodeling during early post-implantation period in mice: investigation of associations with decidual uNK cells and invasive trophoblast. *Biochem. Biophys. Res. Commun.* **417,** 847–852.
22. Raz, R., Avni, T., Neeman, M. 2014. Multimodal imaging of the mouse placenta. In *The Guide to Investigation of Mouse Pregnancy* (B. A. Croy, A. T. Yamada, F. J. DeMayo, S. L. Adamson, eds.), Elsevier Inc., San Diego, CA, 363–372.
23. Avni, R., Neeman, M., Garbow, J. R. (2015) Functional MRI of the placenta: from rodents to humans. *Placenta* **36,** 615–622.
24. Stewart, I., Mukhtar, D. D. (1988) The killing of mouse trophoblast cells by granulated metrial gland cells in vitro. *Placenta* **9,** 417–425.
25. Stewart, I. J. (1990) Granulated metrial gland cells in the mouse placenta. *Placenta* **11,** 263–275.
26. Felker, A. M., Chen, Z., Foster, W. G., Croy, B. A. (2013) Receptors for non-MHC ligands contribute to uterine natural killer cell activation during pregnancy in mice. *Placenta* **34,** 757–764.
27. Stewart, I., Peel, S. (1980) Granulated metrial gland cells at implantation sites of the pregnant mouse uterus. *Anat. Embryol.* (*Berl.*) **160,** 227–238.
28. Pace, D., Morrison, L., Bulmer, J. N. (1989) Proliferative activity in endometrial stromal granulocytes throughout menstrual cycle and early pregnancy. *J. Clin. Pathol.* **42,** 35–39.
29. Natsuaki, Y., Egawa, G., Nakamizo, S., Ono, S., Hanakawa, S., Okada, T., Kusuba, N., Otsuka, A., Kitoh, A., Honda, T., Nakajima, S., Tsuchiya, S., Sugimoto, Y., Ishii, K. J., Tsutsui, H., Yagita, H., Iwakura, Y., Kubo, M., Ng, L., Hashimoto, T., Fuentes, J., Guttman-Yassky, E., Miyachi, Y., Kabashima, K. (2014) Perivascular leukocyte clusters are essential for efficient activation of effector T cells in the skin. *Nat. Immunol.* **15,** 1064–1069.
30. Grakoui, A., Bromley, S. K., Sumen, C., Davis, M. M., Shaw, A. S., Allen, P. M., Dustin, M. L. (1999) The immunological synapse: a molecular machine controlling T cell activation. *Science* **285,** 221–227.
31. Monks, C. R., Freiberg, B. A., Kupfer, H., Sciaky, N., Kupfer, A. (1998) Three-dimensional segregation of supramolecular activation clusters in T cells. *Nature* **395,** 82–86.
32. Brown, A. C., Oddos, S., Dobbie, I. M., Alakoskela, J. M., Parton, R. M., Eissmann, P., Neil, M. A., Dunsby, C., French, P. M., Davis, I., Davis, D. M. (2011) Remodelling of cortical actin where lytic granules dock at natural killer cell immune synapses revealed by super-resolution microscopy (pulished correction available at http://dx.doi.org/10.1371/annotation/cfe6f47e-8c81-4ef0-bdf3-8841cbe40b93). *PLoS Biol.* **9,** e1001152.
33. Springer, T. A., Dustin, M. L. (2012) Integrin inside-out signaling and the immunological synapse. *Curr. Opin. Cell Biol.* **24,** 107–115.
34. Grakoui, A., Bromley, S. K., Sumen, C., Davis, M. M., Shaw, A. S., Allen, P. M., Dustin, M. L. (1999) The immunological synapse: a molecular machine controlling T cell activation. *Science* **285,** 221–227.

35. Olofsson, P. E., Forslund, E., Vanherberghen, B., Chechet, K., Mickelin, O., Ahlin, A. R., Everhorn, T., Onfelt, B. (2014) Distinct migration and contact dynamics of resting and il-2-activated human natural killer cells. *Front. Immunol.* **5,** 80.
36. Kishore, M., Ma, L., Cornish, G., Nourshargh, S., Marelli-Berg, F. M. (2012) Primed T cell responses to chemokines are regulated by the immunoglobulin-like molecule CD31. *PLoS One* **7,** e39433.
37. Ma, L., Cheung, K. C., Kishore, M., Nourshargh, S., Mauro, C., Marelli-Berg, F. M. (2012) CD31 exhibits multiple roles in regulating T lymphocyte trafficking in vivo. *J. Immunol.* **189,** 4104–4111.
38. Kim, S. W., Kim, H., Cho, H. J., Lee, J. U., Levit, R., Yoon, Y. S. (2010) Human peripheral blood-derived $CD31^+$ cells have robust angiogenic and vasculogenic properties and are effective for treating ischemic vascular disease. *J. Am. Coll. Cardiol.* **56,** 593–607.
39. Kushner, E. J., MacEneaney, O. J., Morgan, R. G., Van Engelenburg, A. M., Van Guilder, G. P., DeSouza, C. A. (2010) $CD31^+$ T cells represent a functionally distinct vascular T cell phenotype. *Blood Cells Mol. Dis.* **44,** 74–78.
40. Shortman, K., Heath, W. R. (2010) The $CD8^+$ dendritic cell subset. *Immunol. Rev.* **234,** 18–31.
41. Zarnani, A. H., Moazzeni, S. M., Shokri, F., Salehnia, M., Jeddi-Tehrani, M. (2007) Kinetics of murine decidual dendritic cells. *Reproduction* **133,** 275–283.
42. Moldenhauer, L. M., Keenihan, S. N., Hayball, J. D., Robertson, S. A. (2010) GM-CSF is an essential regulator of T cell activation competence in uterine dendritic cells during early pregnancy in mice. *J. Immunol.* **185,** 7085–7096.
43. Blois, S. M., Barrientos, G., Garcia, M. G., Orsal, A. S., Tometten, M., Cordo-Russo, R. I., Klapp, B. F., Santoni, A., Fernández, N., Terness, P., Arck, P. C. (2008) Interaction between dendritic cells and natural killer cells during pregnancy in mice. *J. Mol. Med.* **86,** 837–852.
44. Cha, J., Bartos, A., Park, C., Sun, X., Li, Y., Cha, S. W., Ajima, R., Ho, H. Y., Yamaguchi, T. P., Dey, S. K. (2014) Appropriate crypt formation in the uterus for embryo homing and implantation requires Wnt5a-ROR signaling. *Cell Reports* **8,** 382–392.
45. Marelli-Berg, F. M., Clement, M., Mauro, C., Caligiuri, G. (2013) An immunologist's guide to CD31 function in T-cells. *J. Cell Sci.* **126,** 2343–2352.
46. Clement, M., Fornasa, G., Guedj, K., Ben Mkaddem, S., Gaston, A. T., Khallou-Laschet, J., Morvan, M., Nicoletti, A., Caligiuri, G. (2014) CD31 is a key coinhibitory receptor in the development of immunogenic dendritic cells. *Proc. Natl. Acad. Sci. USA* **111,** E1101–E1110.
47. Berman, M. E., Xie, Y., Muller, W. A. (1996) Roles of platelet/endothelial cell adhesion molecule-1 (PECAM-1, CD31) in natural killer cell transendothelial migration and beta 2 integrin activation. *J. Immunol.* **156,** 1515–1524.
48. Poggi, A., Panzeri, M. C., Moretta, L., Zocchi, M. R. (1996) CD31-triggered rearrangement of the actin cytoskeleton in human natural killer cells. *Eur. J. Immunol.* **26,** 817–824.
49. Ma, L., Mauro, C., Cornish, G. H., Chai, J. G., Coe, D., Fu, H., Patton, D., Okkenhaug, K., Franzoso, G., Dyson, J., Nourshargh, S., Marelli-Berg, F. M. (2010) Ig gene-like molecule CD31 plays a nonredundant role in the regulation of T-cell immunity and tolerance. *Proc. Natl. Acad. Sci. USA* **107,** 19461–19466.
50. Delgado, S. R., McBey, B. A., Yamashiro, S., Fujita, J., Kiso, Y., Croy, B. A. (1996) Accounting for the peripartum loss of granulated metrial gland cells, a natural killer cell population, from the pregnant mouse uterus. *J. Leukoc. Biol.* **59,** 262–269.
51. Blois, S. M., Alba Soto, C. D., Tometten, M., Klapp, B. F., Margni, R. A., Arck, P. C. (2004) Lineage, maturity, and phenotype of uterine murine dendritic cells throughout gestation indicate a protective role in maintaining pregnancy. *Biol. Reprod.* **70,** 1018–1023.
52. Immunological Genome Consortium. (2015) Transcriptional programs define molecular characteristics of innate lymphoid cell classes and subsets. *Nat. Immunol.* **16,** 306–317.
53. Doisne, J. M., Balmas, E., Boulenouar, S., Gaynor, L. M., Kieckbusch, J., Gardner, L., Hawkes, D. A., Barbara, C. F., Sharkey, A. M., Brady, H. J., Brosens, J. J., Moffett, A., Colucci, F. (2015) Composition, development, and function of uterine innate lymphoid cells. *J. Immunol.* **195,** 3937–3945.
54. Tirado-González, I., Muñoz-Fernández, R., Prados, A., Leno-Durán, E., Martin, F., Abadía-Molina, A. C., Olivares, E. G. (2012) Apoptotic $DC\text{-}SIGN^+$ cells in normal human decidua. *Placenta* **33,** 257–263.
55. Dietl, J., Hönig, A., Kämmerer, U., Rieger, L. (2006) Natural killer cells and dendritic cells at the human feto-maternal interface: an effective cooperation? *Placenta* **27,** 341–347.
56. Leno-Durán, E., Muñoz-Fernández, R., Olivares, E. G., Tirado-González, I. (2014) Liaison between natural killer cells and dendritic cells in human gestation. *Cell. Mol. Immunol.* **11,** 449–455.
57. Chijioke O., Münz C. (2013) Dendritic cell derived cytokines in human natural killer cell differentiation and activation. *Front. Immunol.* 4, article 365. 10.3389.fimmu.2013.000365.
58. Kämmerer, U., Eggert, A. O., Kapp, M., McLellan, A. D., Geijtenbeek, T. B., Dietl, J., van Kooyk, Y., Kämpgen, E. (2003) Unique appearance of proliferating antigen-presenting cells expressing DC-SIGN (CD209) in the decidua of early human pregnancy. *Am. J. Pathol.* **162,** 887–896.
59. Wong, J. L., Berk, E., Edwards, R. P., Kalinski, P. (2013) IL-18-primed helper NK cells collaborate with dendritic cells to promote recruitment of effector $CD8^+$ T cells to the tumor microenvironment. *Cancer Res.* **73,** 4653–4662.
60. Tamzalit, F., Barbieux, I., Plet, A., Heim, J., Nedellec, S., Morisseau, S., Jacques, Y., Mortier, E. (2014) IL-15.IL-15Rα complex shedding following trans-presentation is essential for the survival of IL-15 responding NK and T cells. *Proc. Natl. Acad. Sci. USA* **111,** 8565–8570.
61. Tittarelli, A., Mendoza-Naranjo, A., Farías, M., Guerrero, I., Ihara, F., Wennerberg, E., Riquelme, S., Gleisner, A., Kalergis, A., Lundqvist, A., López, M. N., Chambers, B. J., Salazar-Onfray, F. (2014) Gap junction intercellular communications regulate NK cell activation and modulate NK cytotoxic capacity. *J. Immunol.* **192,** 1313–1319.
62. Bellora, F., Castriconi, R., Dondero, A., Reggiardo, G., Moretta, L., Mantovani, A., Moretta, A., Bottino, C. (2010) The interaction of human natural killer cells with either unpolarized or polarized macrophages results in different functional outcomes. *Proc. Natl. Acad. Sci. USA* **107,** 21659–21664.
63. Co, E. C., Gormley, M., Kapidzic, M., Rosen, D. B., Scott, M. A., Stolp, H. A., McMaster, M., Lanier, L. L., Bárcena, A., Fisher, S. J. (2013) Maternal decidual macrophages inhibit NK cell killing of invasive cytotrophoblasts during human pregnancy. *Biol. Reprod.* **88,** 155.
64. Tilburgs, T., Crespo, A. C., van der Zwan, A., Rybalov, B., Raj, T., Stranger, B., Gardner, L., Moffett, A., Strominger, J. L. (2015) Human $HLA\text{-}G^+$ extravillous trophoblasts: immune-activating cells that interact with decidual leukocytes. *Proc. Natl. Acad. Sci. USA* **112,** 7219–7224.
65. Vacca, P., Cantoni, C., Vitale, M., Prato, C., Canegallo, F., Fenoglio, D., Ragni, N., Moretta, L., Mingari, M. C. (2010) Crosstalk between decidual NK and $CD14^+$ myelomonocytic cells results in induction of Tregs and immunosuppression. *Proc. Natl. Acad. Sci. USA* **107,** 11918–11923.
66. Michel, T., Hentges, F., Zimmer, J. (2012) Consequences of the crosstalk between monocytes/macrophages and natural killer cells. *Front. Immunol.* **3,** 403.
67. Ardolino, M., Zingoni, A., Cerboni, C., Cecere, F., Soriani, A., Iannitto, M. L., Santoni, A. (2011) DNAM-1 ligand expression on Ag-stimulated T lymphocytes is mediated by ROS-dependent activation of DNA-damage response: relevance for NK-T cell interaction. *Blood* **117,** 4778–4786.
68. Zingoni, A., Ardolino, M., Santoni, A., Cerboni, C. (2012) NKG2D and DNAM-1 activating receptors and their ligands in NK-T cell interactions: role in the NK cell-mediated negative regulation of T cell responses. *Front. Immunol.* **3,** 408.
69. Hüber, C. M., Doisne, J.-M., Colucci, F. (2015) IL-12/15/18-preactivated NK cells suppress GvHD in a mouse model of mismatched hematopoietic cell transplantation. *Eur. J. Immunol.* **45,** 1727–1735.
70. Nielsen, N., Ødum, N., Ursø, B., Lanier, L. L., Spee, P. (2012) Cytotoxicity of CD56(bright) NK cells towards autologous activated $CD4^+$ T cells is mediated through NKG2D, LFA-1 and TRAIL and dampened via CD94/NKG2A. *PLoS One* **7,** e31959.
71. Waggoner, S. N., Taniguchi, R. T., Mathew, P. A., Kumar, V., Welsh, R. M. (2010) Absence of mouse 2B4 promotes NK cell-mediated killing of activated $CD8^+$ T cells, leading to prolonged viral persistence and altered pathogenesis. *J. Clin. Invest.* **120,** 1925–1938.
72. Ralainirina, N., Poli, A., Michel, T., Poos, L., Andrès, E., Hentges, F., Zimmer, J. (2007) Control of NK cell functions by $CD4^+CD25^+$ regulatory T cells. *J. Leukoc. Biol.* **81,** 144–153.
73. Pedroza-Pacheco, I., Madrigal, A., Saudemont, A. (2013) Interaction between natural killer cells and regulatory T cells: perspectives for immunotherapy. *Cell. Mol. Immunol.* **10,** 222–229.
74. Kopcow, H. D., Allan, D. S., Chen, X., Rybalov, B., Andzelm, M. M., Ge, B., Strominger, J. L. (2005) Human decidual NK cells form immature activating synapses and are not cytotoxic. *Proc. Natl. Acad. Sci. USA* **102,** 15563–15568.
75. Burke, S. D., Barrette, V. F., Gravel, J., Carter, A. L., Hatta, K., Zhang, J., Chen, Z., Leno-Durán, E., Bianco, J., Leonard, S., Murrant, C., Adams, M. A., Croy, B. A. (2010) Uterine NK cells, spiral artery modification and the regulation of blood pressure during mouse pregnancy. *Am. J. Reprod. Immunol.* **63,** 472–481.
76. Krikun, G., Mor, G., Alvero, A., Guller, S., Schatz, F., Sapi, E., Rahman, M., Caze, R., Qumsiyeh, M., Lockwood, C. J. (2004) A novel immortalized human endometrial stromal cell line with normal progestational response. *Endocrinology* **145,** 2291–2296.
77. Brosens, J. J., Salker, M. S., Teklenburg, G., Nautiyal, J., Salter, S., Lucas, E. S., Steel, J. H., Christian, M., Chan, Y. W., Boomsma, C. M., Moore, J. D., Hartshorne, G. M., Sućurović, S., Mulac-Jericevic, B., Heijnen, C. J., Quenby, S., Koerkamp, M. J., Holstege, F. C., Shmygol, A., Macklon, N. S. (2014) Uterine selection of human embryos at implantation. *Sci. Rep.* **4,** 3894.

KEY WORDS:
implantation site · lymphocyte conjugation · mouse pregnancy
NK cell subsets · T cells · whole-mount in situ immunohistochemistry